Assessing lesion malignancy by scanning small-angle X-ray scattering of breast tissue with microcalcifications

Arboleda, Carolina ; Lütz-Bueno, Viviane ; Wang, Zhentian ; Villanueva-Perez, Pablo ; Guizar-Sicairos, Manuel ; Liebi, Marianne ; Varga, Zsuzsanna ; Stampanoni, Marco

Abstract: Scanning small-angle X-ray scattering (SAXS) measurements were performed on 36 formalin-fixed breast tissue biopsies, obtained from two patients. All samples contained microcalcifications of type II, i.e. formed by hydroxyapatite. We demonstrate the feasibility of classifying breast lesions by scanning SAXS of tissues containing microcalcifications with a resolution of 35 m × 30 m. We report a characteristic Bragg peak found around q=1.725 nmamp;lt;supamp;gt;-1amp;lt;/supamp;gt; that occurs primarily for malignant lesions. Such a clear SAXS fingerprint is potentially linked to structural changes of the breast tissue and correspond to dimensions of about 3.7 nm. Such a material property could be used as an early indicator of malignancy development, as it is readily assessed by SAXS. If this fingerprint is combined with other known SAXS features, which also indicate the level of malignancy, such as lipid spacing and collagen periodicity, it could complement traditional pathology-based analyses. To confirm the SAXS-based classification, a histopathological workup and a gold standard histopathological diagnosis were conducted to determine the malignancy level of the lesions. Our aim is to report this SAXS fingerprint, which is clearly related to malignant breast lesions. However, any further conclusion based on our dataset is limited by the low number of patients and samples. Running a broad study to increase the number of samples and patients is of great importance and relevance for the breast-imaging community.

DOI: https://doi.org/10.1088/1361-6560/ab2c36

Assessing lesion malignancy by scanning small-angle X-ray scattering of breast tissue with microcalcifications

To cite this article before publication: Carolina Arboleda *et al* 2019 *Phys. Med. Biol.* in press https://doi.org/10.1088/1361-6560/ab2c36

Assessing lesion malignancy by scanning small-angle X-ray scattering of breast tissue with microcalcifications

C. Arboleda,[1,2,a)] V. Lutz-Bueno,[1,b)] Z. Wang,[1,2] P. Villanueva-Perez,[1] M. Guizar-Sicairos,[1] M. Liebi,[3,4] Z. Varga,[5] and M. Stampanoni[6,2]

[1)] *Swiss Light Source, Paul Scherrer Institute, 5232 Villigen, Switzerland*
[2)] *ETH Zurich, 8092 Zurich, Switzerland*
[3)] *MAX IV Laboratory, 225 92 Lund, Sweden*
[4)] *Chalmers University of Technology, 412 58 Goeteborg, Sweden*
[5)] *Institute of Pathology and Molecular Pathology, University Hospital Zurich, 8091 Zurich, Switzerland*
[6)] *PSI, 5232 Villigen, Switzerland*

(Dated: 24 June 2019)

Scanning small-angle X-ray scattering (SAXS) measurements were performed on 36 formalin-fixed breast tissue biopsies, obtained from two patients. All samples contained microcalcifications of type II, *i.e.* formed by hydroxyapatite. We demonstrate the feasibility of classifying breast lesions by scanning SAXS of tissues containing microcalcifications with a resolution of 35 μm $\times$ 30 μm. We report a characteristic Bragg peak found around q = 1.725 nm^{-1} that occurs primarily for malignant lesions. Such a clear SAXS fingerprint is potentially linked to structural changes of the breast tissue and correspond to dimensions of about 3.7 nm. Such a material property could be used as an early indicator of malignancy development, as it is readily assessed by SAXS. If this fingerprint is combined with other known SAXS features, which also indicate the level of malignancy, such as lipid spacing and collagen periodicity, it could complement traditional pathology-based analyses. To confirm the SAXS-based classification, a histopathological workup and a gold standard histopathological diagnosis were conducted to determine the malignancy level of the lesions. Our aim is to report this SAXS fingerprint, which is clearly related to malignant breast lesions. However, any further conclusion based on our dataset is limited by the low number of patients and samples. Running a broad study to increase the number of samples and patients is of great importance and relevance for the breast-imaging community.

Keywords: Small-angle X-ray scattering, breast cancer, breast microcalcifications, breast lesion diagnosis

I. INTRODUCTION

Breast cancer is the second most commonly diagnosed cancer among women after skin cancer[1]. Even though several *in situ* and *in vivo* imaging methods are combined to increase the confidence of cancer malignancy level assessment, the accurate diagnosis of cancer remains a challenge and biopsy extraction is often required to confirm whether a breast tissue lesion is benign or malignant. Cancer diagnosis and treatment require a multi-disciplinary team composed of surgeons, pathologists and technicians, to have full access to the clinical history of the patient as well as the biological and structural characteristics of the biopsy sample.

One important predictor of breast cancer is the presence of microcalcifications, which are usually benign deposits of calcium. Orsi et al.[2] suggested that the morphology and distribution of microcalcifications may indicate the malignancy level of breast tissue lesions. Grating interferometry (GI) has been tested on its ability to provide a non-invasive malignancy level assessment based on the microcalcifications type and structure[3–5]. The results of those investigations suggest that measuring scattering interactions can potentially discriminate morphological characteristics that are associated to cancer[4–6].

Insights into the structural organization of biological tissues provide ways to understand how their processes, diseases and functionality develop. Small-angle X-ray scattering (SAXS) is able to provide structural information of noncrystalline materials in the range of tens of micrometers down to a few nanometers[7,8]. If a scanning-based SAXS setup is combined with a focused X-ray beam, two-dimensional maps of the structural changes can be obtained for heterogeneous samples[9–14]. For instance, Siu et al.[15] evaluated the diagnostic potential of SAXS for brain tumors and concluded that this technique can be an effective classifier of malignancy. Giannini et al.[16] evaluated the SAXS and wide-angle X-ray scattering (WAXS) patterns of bone biopsies collected from osteoarthritis-affected patients. After performing principal component and canonical correlation analyses on the SAXS and WAXS data, the nanostructural properties of collagen over extended areas of bone were characterized and quantified. They concluded based on structural changes that there is correlation between age and cross-linking-induced rigidity of collagen fibers.

Among the numerous diseases that provoke structural changes in tissues, the understanding of the formation and the classification of breast cancer with high accuracy

[a)] Electronic mail: carolina.arboleda@psi.ch
[b)] Electronic mail: Viviane.Lutz-Bueno@psi.ch

is of fundamental importance. Fernandez et al.[10] employed SAXS to investigate 28 human breast tumor specimens. Differences between the scattering signals from invasive malignant lesions and healthy regions were observed. Ryan and Farquharson[17] measured Compton and coherent scattering interactions, using an X-ray tube and a high-purity Germanium (HPGe) detector, to classify malignant and benign breast tissue lesions. The scattering spectra were analyzed with a peak-fitting routine and a subsequent multivariate analysis. A sensitivity of 54% and a specificity of 100% were obtained for the dataset. Despite valuable outcomes in breast cancer diagnosis by SAXS, to our knowledge none of them focused specifically on tissue containing microcalcifications, whose presence is known to constitute one of the most important diagnostic markers of breast cancer[18–21]

Here we focus on 36 formalin-fixed human breast tissue samples from two different patients, all containing microcalcifications. Scanning SAXS measurements were performed using a focused X-ray beam with a resolution of 35 μm × 30 μm. The SAXS patterns distributed over millimetric areas of tissue containing embedded microcalcifications served as a base for malignancy level assessment. Thanks to the spatial resolution and coverage provided by scanning SAXS, different sample regions can be resolved. The possibility of distinguishing different types and structures of tissues in regions of a single sample enables a detailed analysis and makes easier to establish a link between malignancy and structural changes of the healthy tissue. Such reliable method could be a valuable candidate to increase the precision of cancer diagnosis and classification. The outcomes of our SAXS data analysis indicate that a diagnosis based on the structural changes of a tissue that contains a microcalcification is promising in the examined range of scattering vectors q = 0.5 - 4 nm^{-1}, especially around q = 1.725 nm^{-1} where a fingerprint was observed. However, it is necessary to increase the number of samples and patients to verify the relevance of the aforementioned findings.

II. MATERIALS AND METHODS

A. Sample preparation

Formalin-fixed human breast tissue samples from two patients were attained from the Institute of Pathology and Molecular Pathology at the University Hospital Zurich. Ethical consent was obtained from both patients. Radiographic measurements were performed to verify if microcalcifications were present. Thin 1 - 2 mm slices were cut in the regions of interest (ROI) where microcalcifications were observed. These slices were further imaged on a setup with a field of view of 10 cm × 5 cm to select smaller ROIs. In total, 36 slices containing microcalcifications were obtained. For scanning SAXS measurements, these slices were fixed on a sample holder using Kapton foil and tape and keeping them embedded in formalin.

B. Scanning SAXS measurements

Scanning SAXS[9] was performed at the cSAXS beamline of the Paul Scherrer Institute. A monochromatic beam of 11.2 keV (λ = 1.107Å) was focused to about 35 μm × 30 μm. For every point in the raster scan, a SAXS pattern was recorded; at the same time, the sample transmission was measured by a diode at the beam stop. Scattering patterns were acquired using a PILATUS 2M[22] detector placed 2.16 m away from the sample. An evacuated flight tube was placed between the sample and detector to reduce absorption and parasitic scattering from air. For fast acquisition, SAXS patterns were recorded in a continuous line scan mode with the sample moving at constant speed along y, while the detector continuously records data (Fig. 1a). The detector was operated with 35 ms exposure time and 5 ms readout time, *i.e.* with a frame rate of 25 Hz. The total scan time was 19.6 hours for all 36 samples (1.5 cm × 1.5 cm in area each), with an X-ray flux of 1.81 ×10^{14} photons/s/mm^2. After these measurements, samples underwent a pathological workup with eosin/hematoxylin to assess their malignancy level[23]. Additionally, the microcalcification chemical type was evaluated based on its birefringence properties[24–26].

C. Scanning SAXS data analysis

The analysis of the data set composed of 36 samples was based on the presence of characteristic peaks, here called fingerprints, in the integrated scattering curves for the accessed experimental q-range of 0.5 - 4 nm^{-1}, as shown in Fig. 1b. Our goal is to classify the samples in the data set in malignant and benign lesions. We name the samples as bipj and mipj, where b stands for benign and m for malignant lesions, while i is the sample number and j is the patient number. As an example, we select sample m9p1. Figure 1b shows four selected scattering curves covering the whole measured q-range, while Fig. 1c zooms in the q-range = 1.67 - 1.75 nm^{-1} where fingerprints were observed. The location of the microcalcifications is clear from the transmission map in Fig. 1d, as the X-ray beam is less transmitted when hitting a microcalcification. Points S1-S4 indicate the positions where the scattering patterns in Fig. 1b and c were measured. Points S1 and S4 are similar as they lay in tissue. As expected from breast tissue[27], a prominent lipid Bragg peak is measured at q = 1.5 nm^{-1} in all samples (see Figs. 1c)[28]. Point S2 hits the microcalcification and higher scattering intensities are measured over the whole q-range. The SAXS fingerprint discussed in this work is observed in S2 and S3, indicating that it occurs not only in regions near, but also in regions far away from the microcalcification. In this example, we compare the az-

imuthally integrated SAXS patterns in regions near the calcification, from which the scattering curve S3 originates displaying a clear peak around 1.725 nm^{-1}. Note that S2 also contains a peak around 1.725 nm^{-1}, but it has a higher baseline due to the high scattering originated by the microcalcification. We restricted our peak finding routine to the q-range = 1.67 - 1.75 nm^{-1}, as shown in Fig. 1c, to avoid lipid and collagen peaks. In this range, we search for the position in q and amplitude A of peaks in the selected q-range by fitting a one-term Gaussian function after baseline subtraction. We search for such peaks in all collected scattering patterns, there-with obtaining a map of their amplitude in each pixel and sample, as shown in Fig. 1e.

The measured breast tissue lesions were classified based on the histopathological diagnosis. From the 36 measured samples, 21 were diagnosed as benign and 15 as malignant lesions. Regarding the chemical composition of the microcalcification, all were classified as hydroxyapatite or type II[24]. The histogram in Fig. 1f shows the distribution of peaks in the selected q-range for the 21 benign samples, while Fig. 1g shows the same for the 15 malignant lesions. Each pixel is assigned a value of 1 if there is a peak, and 0 if there is none. These pixel labels are summed up for all benign or malignant samples for each q-range shown in the histograms. It is clear that the large majority of pixels with such signature peak occurs for malignant samples in the searched q-range. Even though q has a distribution of peak positions in Fig. 1g, the maximum number of peaks is found around 1.725 nm^{-1}, and this is the value we refer to as the fingerprint.

III. RESULTS AND DISCUSSION

For further discussion, the samples were separated into two groups, benign and malignant, according to the histopathological diagnosis. They were not further categorized according to the cancer type or malignancy level, due to the reduced number of samples and patients. The main goal of this study is to test the ability of scanning SAXS to discriminate between benign and malignant lesions. The transmission maps, as well as the peak amplitude maps, as previously discussed in Fig. 1, are shown for benign and malignant lesions in Figs. 2 and 3, respectively. We confirmed that all samples contain microcalcifications, based on the transmission maps shown in Figs. 2a and 3a. Clear microcalcifications are observed in the benign samples shown in Fig. 2a, although the amplitude of peaks in the q-range = 1.67 - 1.75 nm^{-1} do not form clear regions, neither near nor far from the microcalcifications, Fig. 2b, except for sample b21p2. An obvious difference is seen in Fig. 3. By comparing Figs. 3a and 3b, a feature emerges as a Bragg peak around q = 1.725 nm^{-1} with large amplitude. Such features are spatially distributed near and far from the microcalcifications. This fingerprint is associated to most of the malignant samples, except for m1p1, m2p2, m3p2, m4p2 and m5p2. Such a clear spatially-resolved feature, which was revealed without any staining or human interpretation, since it is originated directly from structural changes of the tissue, can be potentially used as a fingerprint for cancer diagnosis. The amplitude maps of the Bragg peaks around q = 1.725 nm^{-1} indicate that structural changes occur to the tissue near and far from the microcalcifications. However, whether the microcalcifications lead to the tissue structural changes or vice versa, remains unclear. Additionally, the fingerprint was absent in 5 out of the 15 malignant samples, which might be related to the corresponding malignancy level (BI-RADS)[2]. Although this fingerprint appeared in samples from both patients, which suggests that it may be patient independent, it is important to recall that the majority of benign specimens belonged to patient 2, whereas most of the malignant samples originated from patient 1. This constitutes a major limitation of this study and more patients are definitely needed to be able to reach a significant conclusion concerning the relevance of this fingerprint.

It can be observed in Fig. 3b that, whereas the top row samples m1-m5 do not display any clear peak amplitude in that q-range, all the other samples exhibit increased peak amplitudes located close to the microcalcifications. Samples m6p1 and m7p1 present peak amplitudes mostly located around the microcalcifications and nowhere else in the tissue, whereas the remaining eight samples display peaks even where no microcalcifications are found. One hypothesis is that the Bragg peak at q = 1.725 nm^{-1} is a consequence of tissue structural remodeling induced by cancer and that the microcalcifications are somewhat responsible for this process. The reason why some microcalcifications do not generate such structural change in the tissue, as it is the case for samples m1-m5 as well as for the benign ones, is a potential study that could correlate this fingerprint with microcalcification nanostructure and morphology.

Two receiver-operating characteristic (ROC) curves[29] were calculated, shown in Fig. 4, to find the best threshold to classify benign and malignant lesions using either the presence of peaks or the sum of peak amplitudes per sample (Fig. 2d and 2e) in the q = 1.67-1.75 nm^{-1} range as metric. In the former case, the pixel value was set to 1 where a peak was found and 0 otherwise. Afterwards, the sensitivity, also known as true positive rate (TPR), and specificity, also known as true negative rate (TNR), were calculated as follows:

$$TPR = \frac{TP}{P}, \tag{1}$$

$$TNR = \frac{TN}{N}, \tag{2}$$

where TP, P, TN and N, are the true positives, positives, true negatives and negatives, respectively. The Youden

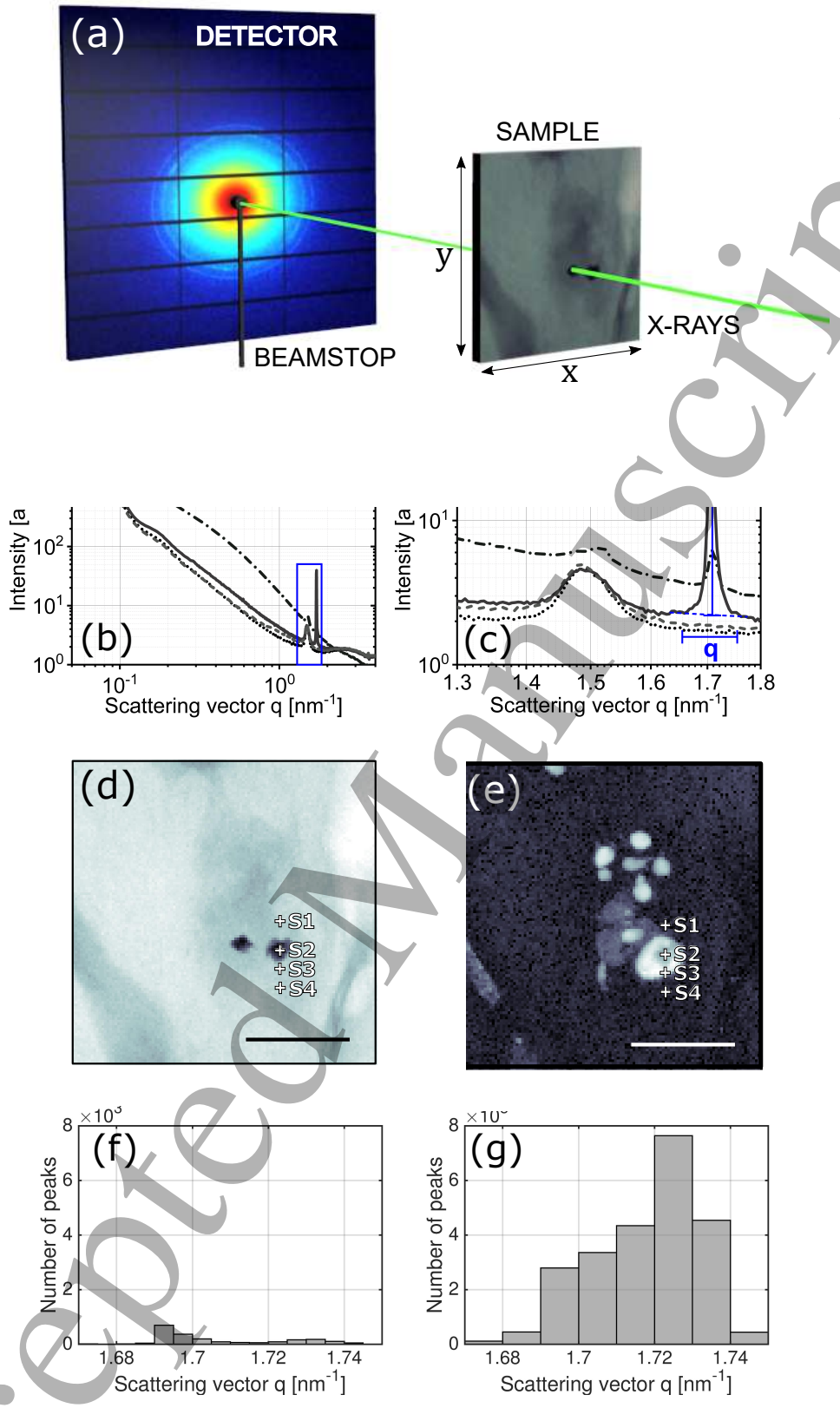

FIG. 1. (a) Experimental setup: The sample is scanned across an X-ray beam along x and y. Scattering patterns are measured by a 2D detector at each scan point. The beamstop is equipped with a diode to simultaneously measure the sample's transmission. (b) Azimuthal integration of points S1-S4 covering the experimental q-range. (c) Zoom in the q-range = 1.3 - 1.8 nm^{-1}, where the amplitudes A of the peaks were extracted in the indicated q-range = 1.67 - 1.75 nm^{-1}, after baseline subtraction. (d) Transmission map of sample m9p1. (e) Map of the amplitude of the peaks in the q-range = 1.67 - 1.75 nm^{-1} of sample m9p1. Points S1-S4 indicate the location of the scattering patterns shown in (b). (f) Histogram of all occurrences of peaks in the q-range = 1.67 - 1.75 nm^{-1} for the 21 benign lesion samples. (g) Histogram of all occurrences of peaks in the q-range = 1.67 - 1.75 nm^{-1} for the 15 malignant lesion samples. The scale bar corresponds to 1 mm.

index (sensitivity+specificity-1)[29] was used to define the optimal cutoff values in both cases and the outcomes are summarized in table I.

TABLE I. Sensitivity and specificity at the optimal cutoff value (Youden index)

Method	Sensitivity	Specificity
Peak presence	60%	100%
Sum of peak amplitudes	67%	100%

The specificity of 100% generated by the presence of a peak at q = 1.725 nm^{-1} indicates a high potential for breast cancer diagnosis for samples containing microcalcifications. The obtained specificity value bespeaks that there is no risk of false positives, while the sensitivity one indicates that up to 40 % of the cancerous cases will be missed if only the peak-presence detection criterion is employed. If the sum of peak amplitudes is considered instead, a 7 % increase in sensitivity can be obtained.

The structural changes related to this SAXS fingerprint could be related to the formation of fibrous tissue. It is known that healthy breast tissue is formed either by evenly dispersed or well-ordered cells. In either case, there are no extraneous proliferation or foreign materials present. A cancerous tumour is formed when excessive accumulation of abnormal cells occur. In vivo Magnetic Resonance Spectroscopy (MRS) studies[31–33] showed that the water-to-fat ratio was higher in invasive ductal carcinomas compared to benign lesions or normal breast parenchyma[31,33,34]. An ex-vivo Nuclear Magnetic Resonance (NMR) investigation further confirmed this finding by demonstrating that malignant carcinosarcoma tissue has higher amounts of water content, which is directly related to fibrous tissue, compared to normal healthy tissue[30]. Since cancerous regions have the tendency to contain more fibrous tissue and water, the peak around q = 1.725 nm^{-1} could correspond to such a structural change[17], and it might explain why this peak is only predominant in malignant lesions.

The diagnosis based on the fingerprint at q = 1.725 nm^{-1} is only known for samples containing microcalcifications, and it could be complementary of other SAXS fingerprints previously reported. Most SAXS studies of human tissues relate abnormalities on collagen structure to the level of malignancy of tumors. For example, the degradation of collagen is associated with invasive carcinoma in breast tissue. This exhibits itself as disperse collagen bundles that break the order of normal tissue. Collagen fibril degradation is associated to the presence of an acidic collagen component that causes collagen chain modifications[35–37]. The collagen degradation is seen in SAXS signals as the axial peaks of collagen become less intense and broader, due to the decrease of ordering with malignancy[38]. Another known SAXS fingerprint is the longitudinal arrangement of collagen fibrils, which gives rise to axial d-spacing peaks that can be used to classify breast tissue types[39–43]. Small displacements of the position of the lipid Bragg peak along q was indicated as a possible SAXS fingerprint for breast cancer diagnosis by Castro et al.[28]. Combining collagen, lipids and fibrous tissue SAXS fingerprints could expand the reliable tools available for cancer diagnosis, as well as level of malignancy assessment (BI-RADS)[2]. If scanning SAXS could be employed not only for classification, but also for BI-RADS categorization, it could become an excellent complement to histo-pathological workups.

IV. CONCLUSION

We analyzed a set of 36 formalin-fixed human breast tissue samples from two different patients by scanning SAXS. The search and classification of fingerprints indicate that it might be possible to classify benign and malignant lesions based on the scattering signals from tissues containing microcalcifications. The presence of a Bragg peak around q = 1.725 nm^{-1} generated a specificity of 100% and a sensitivity of up to 67% when the sum of peak amplitudes is considered per sample, to classify between benign and malignant lesions. Notwithstanding, it is important to recall that a limited number of samples from only two different patients were measured and that the majority of the malignant samples originated from one of the patients, which implies that more samples and patients are definitely required to reach more solid conclusions, including malignant lesions without microcalcifications. It is important to emphasize the added benefit of the spatial-resolution from scanning SAXS for the differentiation of the structural changes of tissue upon the growth of a tumor around a microcalcification. The fact that the scattering is not integrated over the whole sample volume allows discrimination between different sample regions. After this report, deeper investigations to link such a fingerprint to structural changes in breast tissue, as well as the BI-RADS level of cancer, would be essential to understand the development of cancer and its dependency on microcalcifications. Nevertheless, a potential SAXS fingerprint has been identified in malignant breast tissue lesions, which might offer potential in diagnostics as well as in the understanding of structural changes leading to breast cancer.

It is still not certain whether the microcalcifications themselves induce or are related to the structural tissue changes that lead to the peak at q = 1.725 nm^{-1}, observed in malignant lesions. Whether the calcium deposits lead to tissue structural changes, or the tissue structural changes lead to calcium deposits, remains uncertain.

An important limitation of this study is the use of formalin for sample preparation, which can affect the collagen structure in the tissue and cause further degradation and dehydration, influencing SAXS structural analysis[44].

As future work, we plan to measure fresh tissue samples, with and without microcalcifications, to remove the influence of formalin on collagen and combine all known

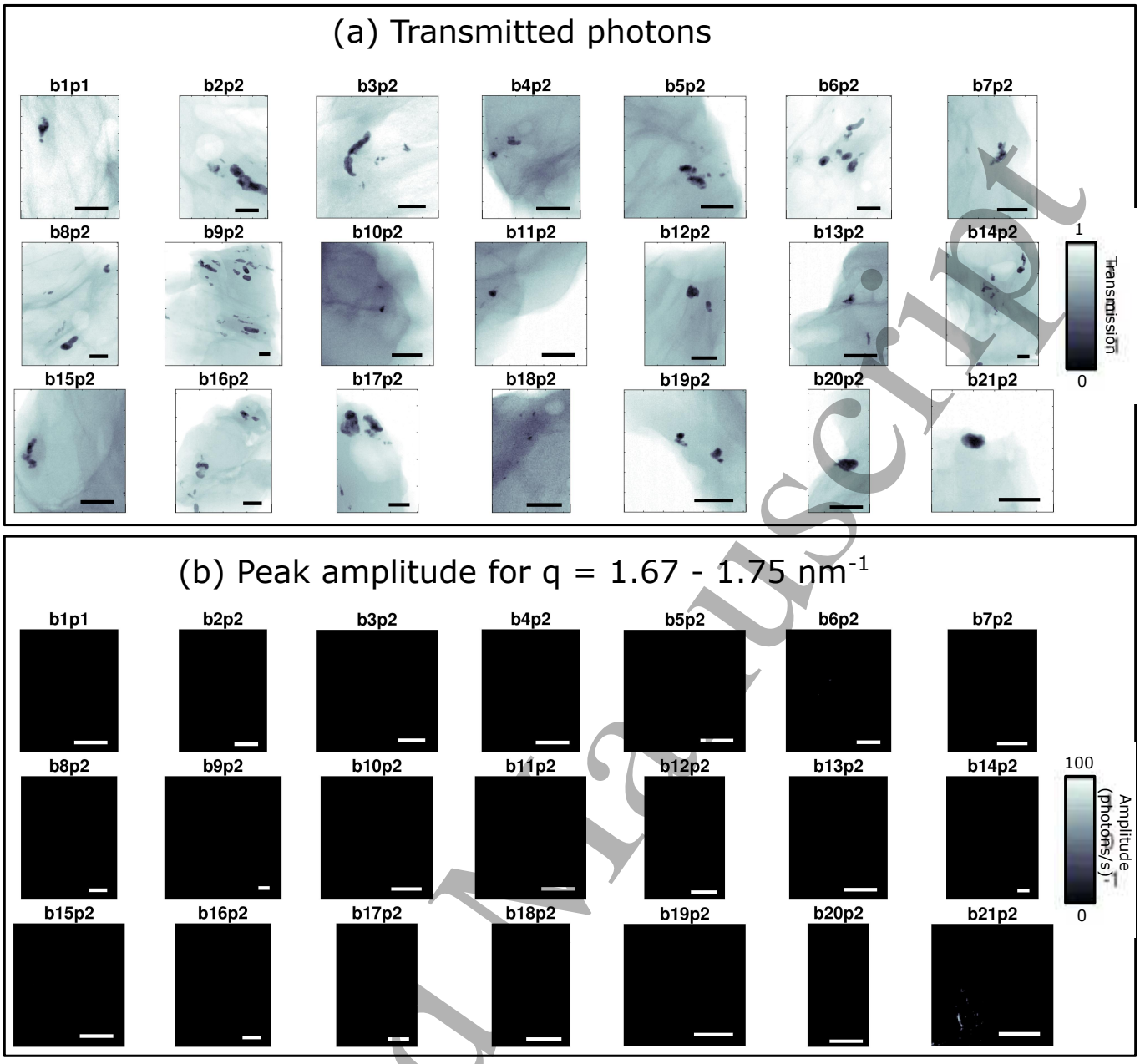

FIG. 2. **Benign lesions measured by scanning SAXS:** (a) Sample transmission maps. (b) Maps of the intensity of the peaks in the q-range = 1.67 - 1.75 nm^{-1}. The scale bars corresponds to 1 mm.

SAXS fingerprints, collagen, lipid, and the possible fibrous tissue, for malignancy level assessment. Additionally, measurements of samples with type I microcalcifications, formed by calcium oxalate, in the q-range covered in this work, are essential to include the scattering of their crystalline configuration as an additional potential fingerprint for breast cancer classification. An interesting next step would be to measure the scattering signals of microcalcification-containing samples with GI, which does not require a synchrotron and can be carried out with a regular X-ray tube, to test whether the information in the q ranges accessible by this technique also allows a benign-malignant lesion discrimination and potentially a BI-RADS categorization[4,5].

V. ACKNOWLEDGMENT

The authors acknowledge the European Research Council (ERC) (ERC-2012-StG 310005-PhaseX) and the Swiss National Foundation (SNF)-Sinergia CRSII2-154472 MedXPhase and CRSII5-183568 for funding this work. They also thank Dr. Andreas Menzel from the the cSAXS beamline at the Swiss Light Source for his critical

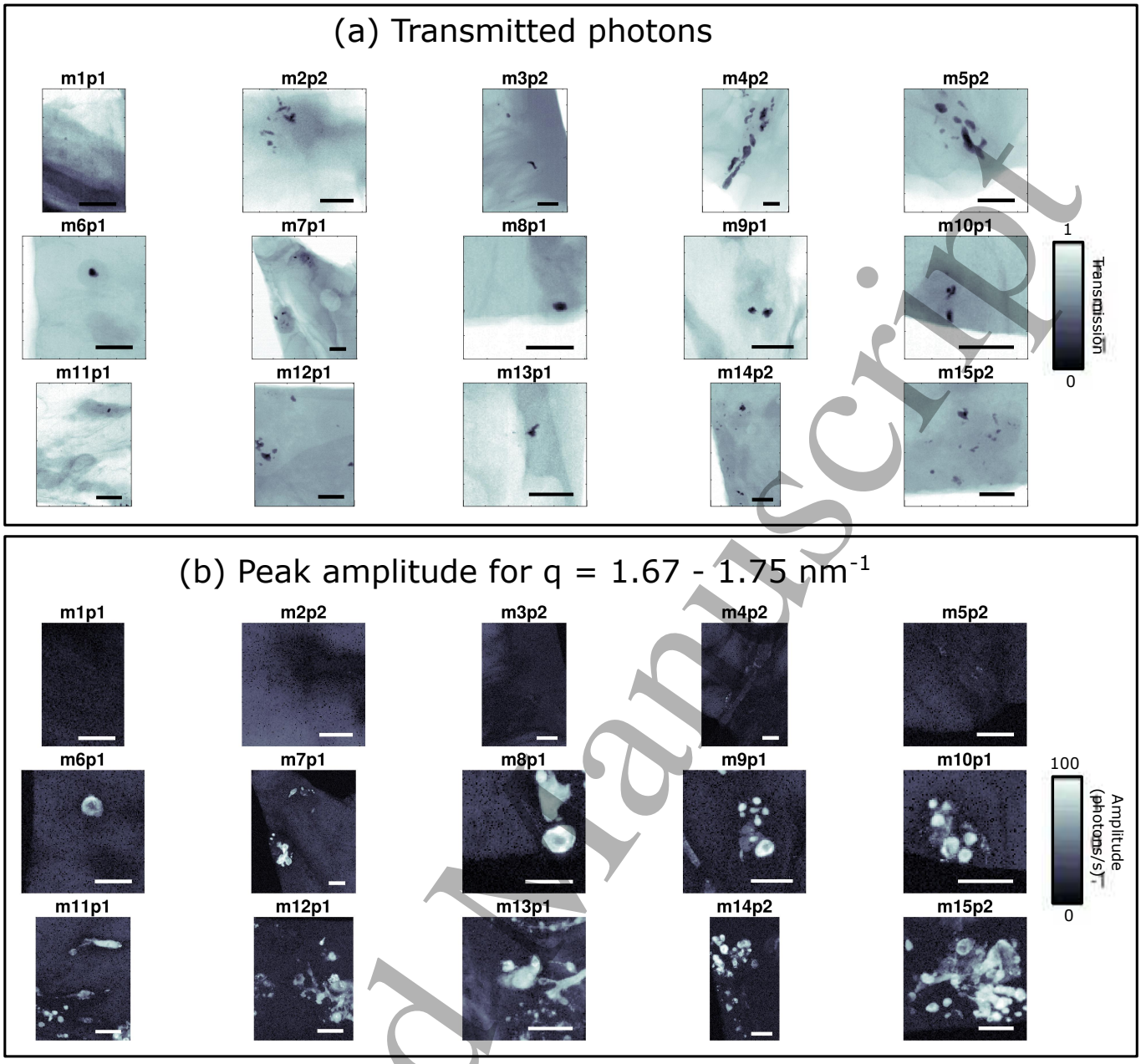

FIG. 3. **Malignant lesions measured by scanning SAXS:** (a) Maps of the relative transmitted photons. (b) Maps of the intensity of the peaks in the q-range = 1.67 - 1.75 nm^{-1}. The scale bars corresponds to 1 mm.

comments on the manuscript.

[1]Breast cancer statistics. Available from internet: http://www.wcrf.org/int/cancer-facts-figures/data-specific-cancers/breast-cancer-statistics (visited 07.08.2017)
[2]DOrsi CJ et al 2003 *Breast Imaging Reporting and Data System (BI-RADS): ACR BI-RADSMammography 4th edn* (American College of Radiology)
[3]Michel T et al 2013 On a dark-field signal generated by micrometer-sized calcifications in phase-contrast mammography *Phys. Med. Biol.*, **58(8)** 2713
[4]Scherer K et al 2015 Toward Clinically Compatible Phase-Contrast Mammography *PLoS ONE* **10(6)** e0130776
[5]Wang Z, Hauser N, Singer G, Trippel M, Kubik-Huch R, Schneider C and Stampanoni M 2014 Non-invasive classification of microcalcifications with phase-contrast X-ray mammography *Nat. Comm.* **5** 1–9
[6]Wang Z, Hauser N, Singer G, Trippel M, Kubik-Huch R, Schneider C and Stampanoni M 2016 Correspondence: Reply to Quantitative evaluation of X-ray dark-field images for microcalcification analysis in mammography *Nat. Comm.* **7** 10868
[7]Glatter, Otto, and Otto Kratky, eds. Small angle X-ray scattering. Academic press, 1982
[8]Narayanan T 2009 High brilliance small-angle X-ray scattering applied to soft matter Current opinion in colloid and interface Science **14(6)** 409–415

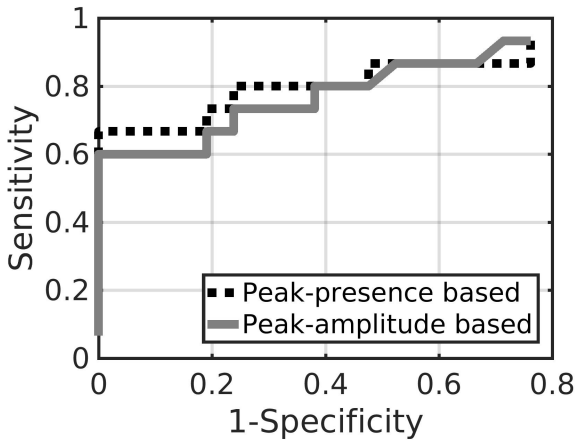

FIG. 4. Receiver operating characteristic (ROC) curves using the presence of peaks (dotted line) or the amplitude of the peaks (solid line) as a criterion to classify benign and malignant breast tissue lesions.

[9]Bunk O, Bech M, Jensen TH, Feidenhans R, Binderup T, Menzel A and Pfeiffer F 2009 Multimodal x-ray scatter imaging *New J. Phys.* **11(12)** 123016

[10]Fernandez M et al 2005 Human breast cancer in vitro: matching histo-pathology with small-angle x-ray scattering and diffraction enhanced x-ray imaging *Phys. Med. Biol.* **50(13)** 2991

[11]Fratzl P, Jakob HF, Rinnerthaler S, Roschger P and Klaushofer K 1997 Position-resolved small-angle X-ray scattering of complex biological materials *J. Appl. Crystallogr.* **30(5)** 765–769

[12]Gourrier A, Wagermaier W, Burghammer M, Lammie D, Gupta HS, Fratzl P, Riekel C, Wess TJ and Paris O 2007 Scanning X-ray imaging with small-angle scattering contrast *Applied Crystallography* **40(s1)** s78-s82

[13]Paris O, Loidl D, Peterlik H, Mueller M, Lichtenegger H and Fratzl P 2000 The internal structure of single carbon fibers determined by simultaneous small-and wide-angle scattering *J. Appl. Crystallogr.* **33(3)** 695–699

[14]Rinnerthaler S, Roschger P, Jakob HF, Nader A, Klaushofer K and Fratzl P 1999 Scanning small angle X-ray scattering analysis of human bone sections *Calcified tissue international* **64(5)** 422–429

[15]Siu KKW et al 2005 Identifying markers of pathology in SAXS data of malignant tissues of the brain *Nuclear Instruments and Methods in Physics Research Section A: Accelerators, Spectrometers, Detectors and Associated Equipment* **548(1)** 140–146

[16]Giannini C et al 2014 Scanning SAXS–WAXS microscopy on osteoarthritis-affected bonean age-related study *J. Appl. Crystallogr.* **47(1)** 110-117

[17]Ryan EA and Farquharson MJ 2007 Breast tissue classification using x-ray scattering measurements and multivariate data analysis *Phys. Med. Biol.* **52(22)** 6679

[18]American College of Radiology (ACR). Breast imaging reporting and data system (BI-RADS), breast imaging atlas. 4th ed., Reston,Va, Am College Radiology, 1259 (2003)

[19]Winchester DP, Jeske JM and Goldschmidt RA 2000 The diagnosis and management of ductal carcinoma in situ of the breast *Am. Cancer J. Clin.* **50(3)** 184

[20]Schreer I and Luttges J 2001 Breast cancer: early detection *Eur. J. Radiol.* **11 (Suppl 2)** S307-S314

[21]Stephen A and Feig MD 2000 Ductal carcinoma in situ. Implications for screening mammography *Radiol. Clin. N. Am.* **38(4)** 653-668

[22]Henrich B, Bergamaschi A, Broennimann C, Dinapoli R, Eikenberry EF, Johnson I, Kobas M, Kraft P, Mozzanica A and Schmitt B 2009 PILATUS: A single photon counting pixel detector for X-ray applications *Nuclear Instruments and Methods in Physics Research Section A: Accelerators, Spectrometers, Detectors and Associated Equipment* **607(1)** 247–249

[23]CSH Protocols; 2008; doi:10.1101/pdb.prot4986

[24]Frappart L et al 1984 Structure and composition of microcalcifications in benign and malignant lesions of the breast: study by light microscopy, transmission and scanning electron microscopy, microprobe analysis, and X-ray diffraction *Hum. Pathol.* **15(9)** 880–889

[25]Radi MJ 1989 Calcium oxalate crystals in breast biopsies. An overlooked form of microcalcification associated with benign breast disease *Archives of pathology laboratory medicine* **113(12)** 1367–1369

[26]Haka AS, Shafer-Peltier KE, Fitzmaurice M, Crowe J, Dasari RR and Feld MS 2002 Identifying microcalcifications in benign and malignant breast lesions by probing differences in their chemical composition using Raman spectroscopy *Cancer research* **62(18)** 5375–5380

[27]Sidhu S, Falzon G, Hart SA, Fox JG, Lewis RA and Siu KKW 2011 Classification of breast tissue using a laboratory system for small-angle x-ray scattering (SAXS) *Phys. Med. Biol.* **56(21)**

[28]Castro CRF, Barroso RC and Lopes RT 2005 Scattering signatures for some human tissues using synchrotron radiation *X-Ray Spectrometry* **34** 477–480

[29]Hajian-Tilaki K 2013 Receiver Operating Characteristic (ROC) Curve Analysis for Medical Diagnostic Test Evaluation *Caspian Journal of Internal Medicine* **4(2)** 627–635

[30]Kiricuta IC , Simplaceanu V 1975 Tissue water content and nuclear magnetic resonance in normal and tumor tissues *Cancer Res.* **35** 1164–1167

[31]Thakur SB, Bartella L, Ishill NM, Morris EA, Liberman L, Dershaw DD, Hricak H, Koutcher JA, Huang W 2006 Comparisons of water-to- fat ratios in malignant, benign breast lesions, and normal breast parenchyma: an in vivo proton MRS study *Proceedings of the 14th Annual Meeting of ISMRM, Seattle*

[32]Thakur SB, Bartella L, Ishill NM, Morris EA, Liberman L, Dershaw DD, Hricak H, Koutcher JA, Huang W 2006 Discrimination of choline- positive invasive breast carcinomas using water-to-fat ratio: a proton MRS study *Proceedings of the 14th Annual Meeting of ISMRM, Seattle*

[33]Jagannathan NR, Singh M, Govindaraju V, Raghunathan P, Coshic O, Julka PK, Rath GK 1998 Volume localized in vivo proton MR spectroscopy of breast carcinoma: variation of water-fat ratio in patients receiving chemotherapy *NMR Biomed.* **11** 414–422

[34]Sharma U, Kumar M, Sah RG and Jagannathan NR 2009 Study of normal breast tissue by in vivo volume localized proton MR spectroscopy: variation of water-fat ratio in relation to the heterogeneity of the breast and the menstrual cycle *Magn. Reson. Imaging* **27** 785–791

[35]Pucci Minafra I, Luparello C, Sciarrino S, Tomasino RM and Minafra S 1985 Quantitative determination of collagen types present in the ductal infiltrating carcinoma of human mammary gland *Cell Biology International Reports* **9** 291–296

[36]Pucci Minafra I, Minafra S, Tomasino RM, Sciarrino S and Tinervia R 1986 Collagen changes in the ductal infiltrating (scirrhous) carcinoma of the human breast. A possible role played by type I trimer collagen on the invasive growth *Journal of Submicroscopic Cytology* **18** 795–805

[37]Rajkumar L, Balasubramanian K, Arunakaran J, Govindarajulu P and Srinivasan N 2005 Influence of estradiol on mammary tumour collagen solubility in DMBA-induced rat mammary tumours *Cell Biology International* **30** 164–168

[38]Suhonen H, Fernndez M, Serimaa R and Suortti P 2005 Simulation of small-angle x-ray scattering from collagen fibrils and comparison with experimental patterns *Phys. Med. Biol.* **50** 5401–5416

[39]A.R. Round, "Ultra-structural analysis of breast tissue", Cranfield University, Cranfield, United Kingdom (2006).

[40] Lewis RA, Rogers KD, Hall CJ, Towns-Andrews E, Slawson S, Evans A, Pinder SE, Ellis IO, Boggis CRM, Hufton AP and Dance DR 2000 Breast cancer diagnosis using scattered X-rays *J. Synchrotron Radiat.* **7** 348–352

[41] Fernandez M, Keyrilainen J, Serimaa R, Torkkeli M, Karjalainen-Lindsberg ML, Tenhunen M, Thomlinson W, Urban V and Suortti P 2002 Small-angle x-ray scattering studies of human breast tissue samples *Phys. Med. Biol.* **47** 577–592

[42] Fernandez M, Keyrilainen J, Karjalainen-Lindsberg ML, Leidenius M, Von Smitten K, Fiedler S and Suortti P 2004 Human breast tissue characterisation with small-angle X-ray scattering *Spectroscopy* **18** 167–176

[43] Changizi V, Oghabian MA, Speller R, Sarkar S and Kheradmand AA 2005 Application of small angle x-ray scattering (SAXS) for differentiation between normal and cancerous breast tissue *International Journal of Medical Sciences* **2** 118–121

[44] Sidhu S 2009 *Small Angle X-ray Scattering as a Diagnostic Tool for Breast Cancer* (Monash: Monash University)